UCAR COMMUNITY PROGRAMS

COSMIC

GPS RO processing from raw phase and amplitude to bending angle

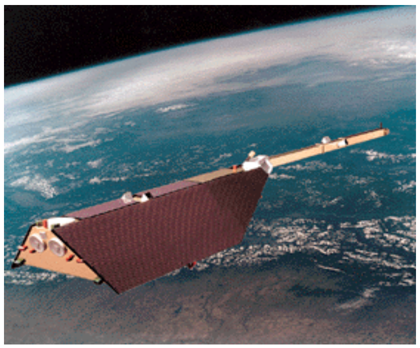

Bill Schreiner
S. Sokolovskiy, C. Rocken, D. Hunt, B. Kuo

UCAR COSMIC Program Office
www.cosmic.ucar.edu

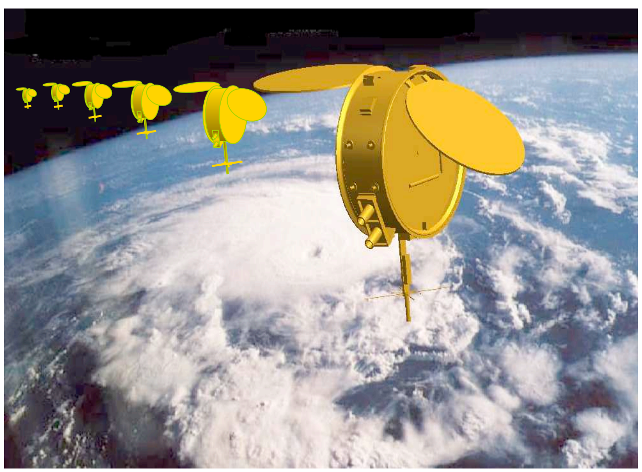

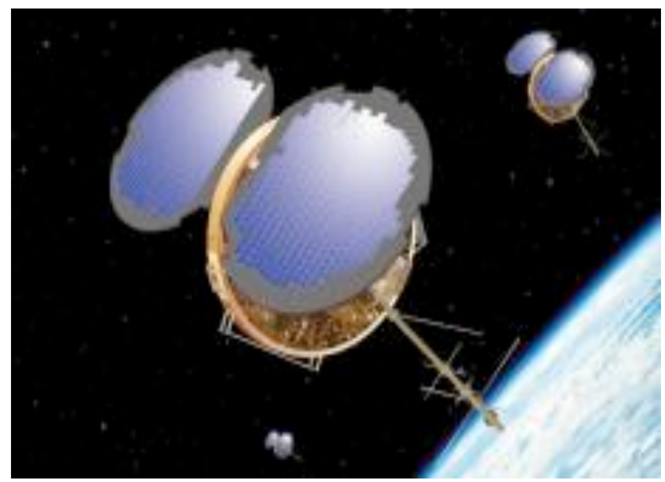

Sept 6-10, 2010 OPAC 2010 Graz, Austria

Outline

- Processing overview
- POD overview and results
- Atmospheric excess phase processing
- Bending angle computation/uncertainty
  - Geometric Optics
  - Wave Optics
- Summary

GPS Radio Occultation

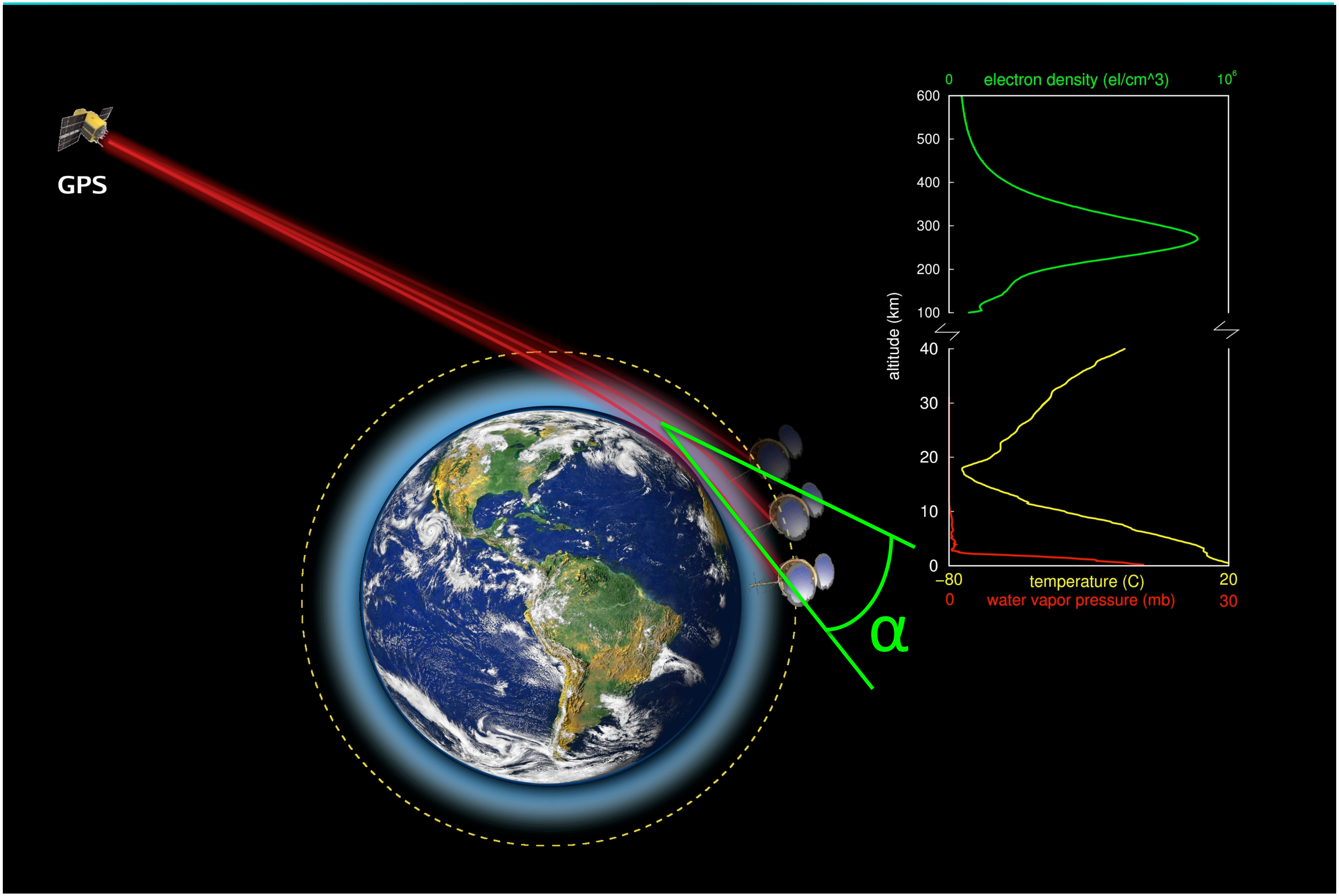

Atmospheric excess phase

- Difference between true phase path between $\vec{r}_1$ *and* $\vec{r}_2$ and straight line (vacuum) path

$$S_{true} - S_{str} = \int n dl - \left| \vec{r}_1 - \vec{r}_2 \right|$$

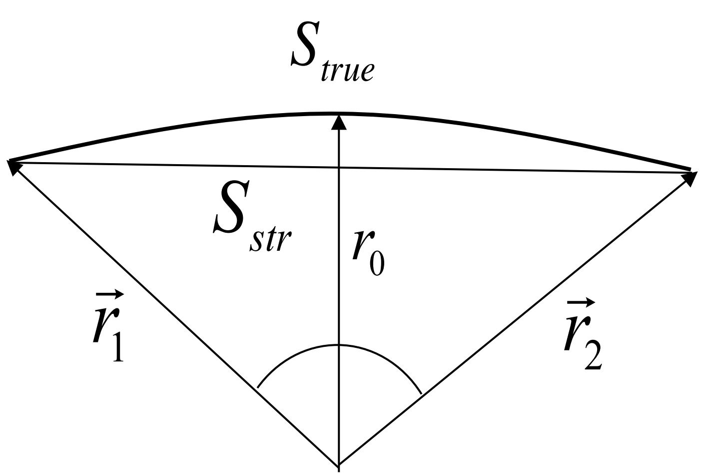

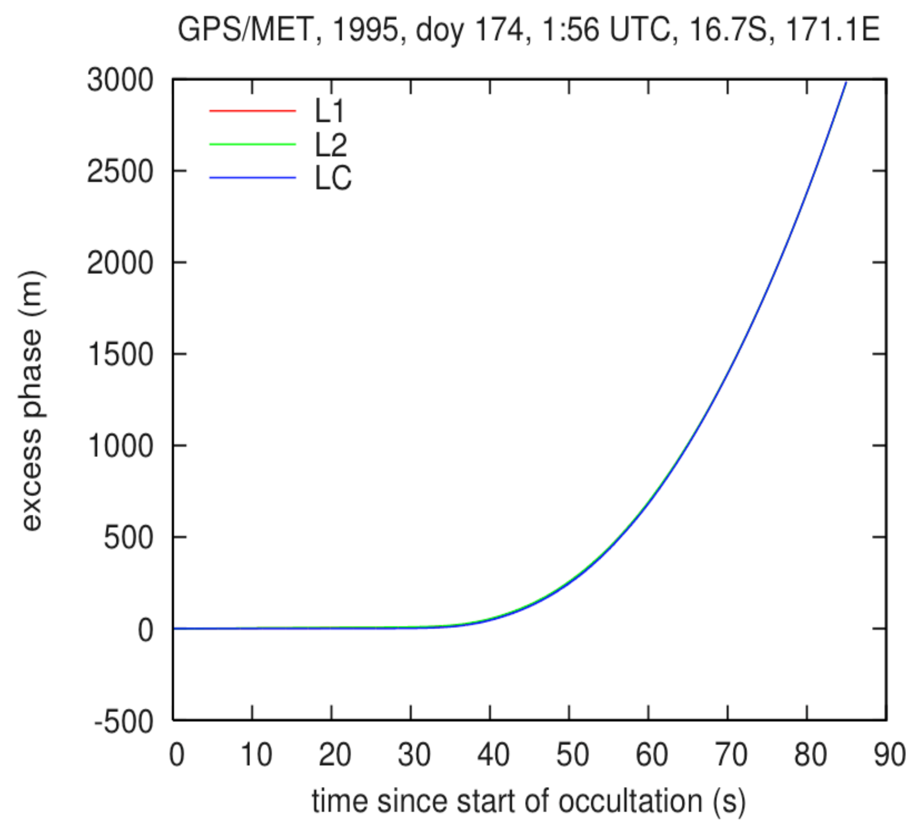

Observation Modeling

$$L1_r^s(t_r) = c \cdot \delta t_r(t_r) + c \cdot \delta t_{r,rel}(t_r) + \rho_r^s(t_r) + \delta\rho_{r,rel}^s(t_r) + c \cdot \delta t^s(t_r - \tau_r^s) + c \cdot \delta t_{rel}^s(t_r - \tau_r^s) + \boxed{\delta\rho_{r,ion}^s(t_r) + \delta\rho_{r,trop}^s(t_r)} + \lambda_1 \cdot N_{amb} + \varepsilon \quad (1)$$

Excess phase

t_r	receive time
c	speed of light in vacuum (m/s)
δt_r	offset between receiver time and proper time at receive time
$\delta t_{r,rel}$	offset between proper time and coordinate time at the receiver due to special and general relativity
ρ_r^s	geometric range at receive time
δt^s	offset between proper time and satellite time at transmit time
δt_{rel}^s	offset between coordinate time and proper time at satellite
$\delta\rho_{r,rel}^s$	gravitational delay between receiver and satellite
τ_r^s	light travel time in vacuum, $\tau_r^s = \rho_r^s(t_r)/c + \delta\rho_{r,rel}^s(t_r)$
$\delta\rho_{r,ion}^s$	ionospheric delay between receiver and satellite
$\delta\rho_{r,trop}^s$	tropospheric delay between receiver and satellite
λ_1	wavelength of L1 signal (m)
N_{amb}	phase ambiguity
ε	phase noise

+ System delays
+ Local spacecraft multipath
+ Antenna phase center offsets and variations
+ Carrier phase wind-up

(Schreiner et al., 2009)

Processing Overview

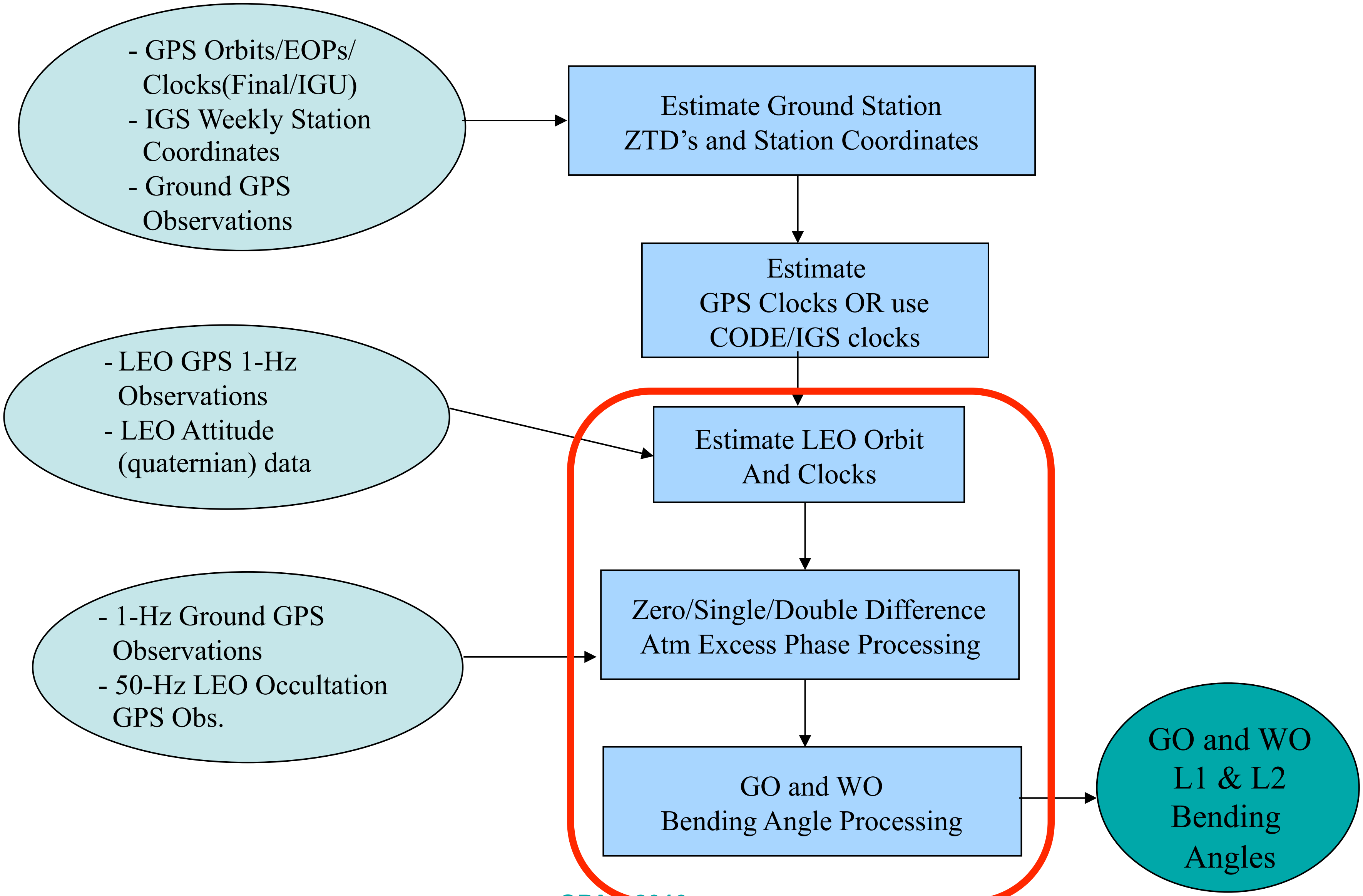

LEO POD at CDAAC with Bernese v5.0

- Zero-Difference ionosphere-free carrier phase observables with reduced-dynamic processing (Svehla and Rothacher, 2003)

$$L3_r^s(t_r) = c_1 \cdot L1_r^s(t_r) - c_2 \cdot L2_r^s(t_r)$$

- Dynamic Model: Gravity - EIGEN1S, Tides - (3rd body, solid Earth, ocean)
- State Parameters:
  - 6 initial conditions (Keplerian elements)
  - 9 solar radiation pressure parameters (bias and 1 cycle per orbital revolution accelerations in radial, transverse, and normal directions)
  - pseudo-stochastic velocity pulses in R-T-N directions every 12 minutes
  - real valued ambiguities
  - LEO clock offset
- Quality Control
  - Post-fit residuals
  - Internal overlaps

COSMIC Post-Processed External Overlaps

- Inter-Agency (UCAR,NCTU,GFZ,JPL) orbit differences
- FM’s 1-6, 2006.216-218, no data gaps, good attitude control

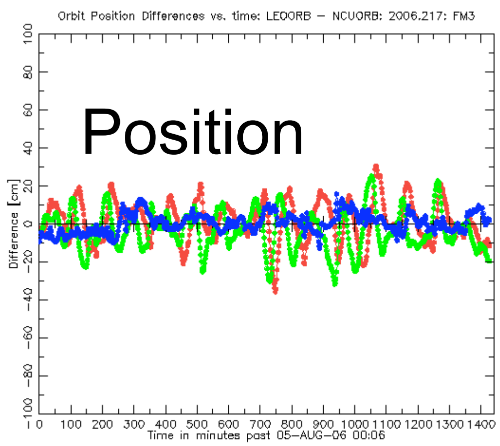

Radial
Along-track
Cross-track

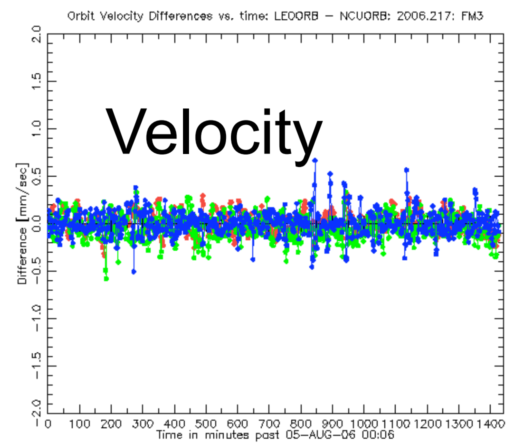

	Radial POS [cm] VEL [mm/s]	**Along-Track** POS [cm] VEL [mm/s]	**Cross-Track** POS [cm] VEL [mm/s]	**3-D RSS** POS [cm] VEL [mm/s]
UCAR - NCTU	8.8 0.13	10.5 0.14	10.5 0.18	17.3 0.26
UCAR - GFZ	9.8 0.15	14.7 0.13	15.0 0.12	23.2 0.23
UCAR - JPL	8.2 0.11	13.1 0.13	9.8 0.13	18.3 0.22

(Schreiner et al., 2009)

COSMIC's Bad Attitude

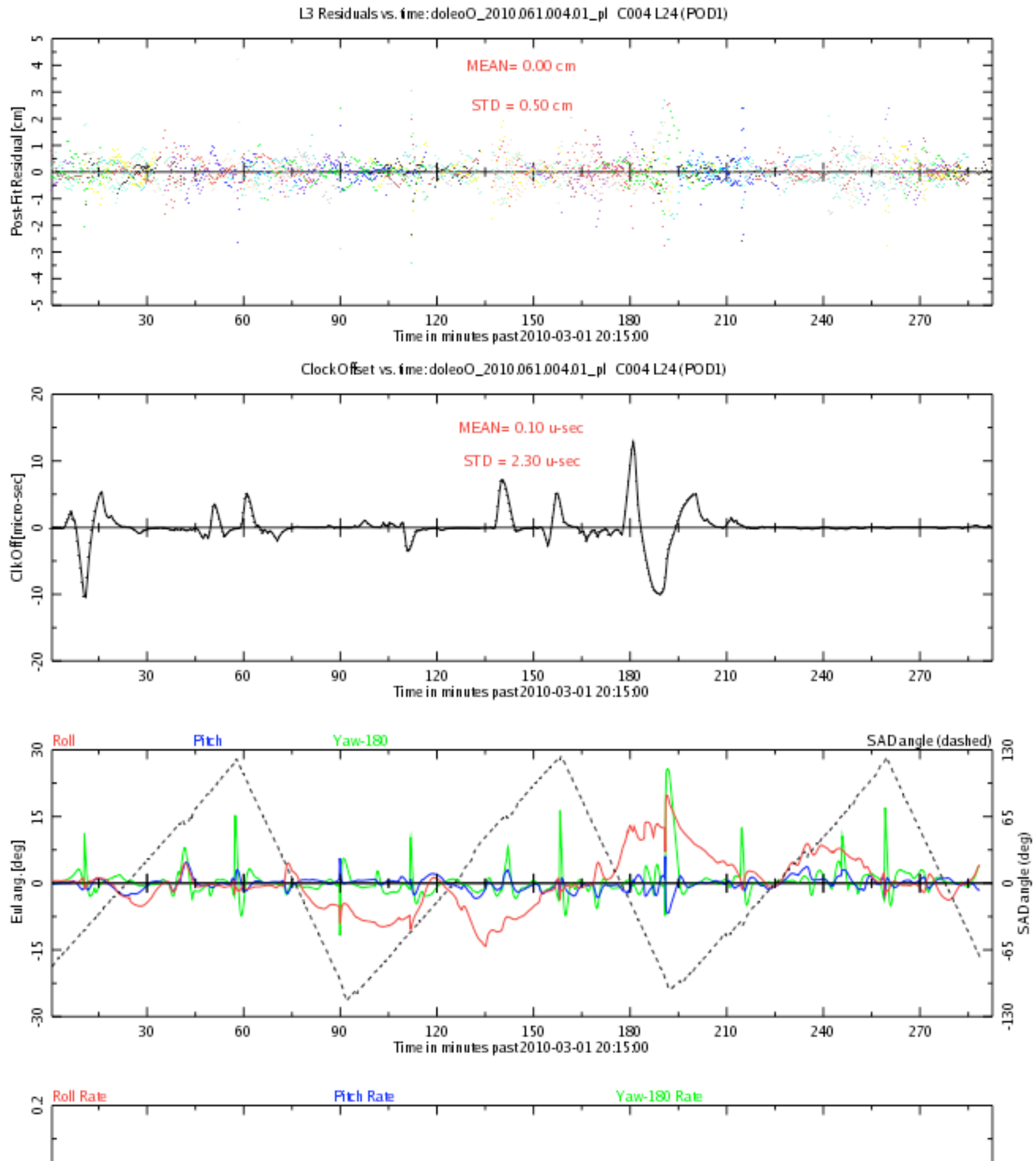

METOP/GRAS Post-Processed External Overlaps

UCAR – EUMETSAT (2007.274-305)

	Radial POS [cm] (VEL: [mm/s])	**Along-Track** POS [cm] (VEL: [mm/s])	**Cross-Track** POS [cm] (VEL: [mm/s])	**3-D RSS** POS [cm] (VEL: [mm/s])
Mean	0.7 (-0.01)	0.9 (-0.01)	2.9 (0.00)	-
STD	4.2 (0.05)	6.0 (0.08)	4.1 (0.04)	8.6 (0.08)

- POD quality
  - COSMIC ~ 15-20 cm (0.15-0.2 mm/s) 3D RMS
  - METOP/GRAS < 10 cm (0.1 mm/s) 3D RMS

Velocity error of 0.1 mm/s results in bending angle error of ~3e-8 rad

Computation of excess atmospheric phase

- Double-Difference
  - Ground/LEO clock fluctuations removed
  - Maximal noise: Fid. site MP, atmos. noise, thermal noise
- Single-Difference
  - LEO clock fluctuations removed
  - Use solved-for GPS clocks to minimizes ground station errors
  - Noise from reference link
- Zero-Difference
  - Assume LEO/USO clock perfect
  - Use solved-for GPS clocks
  - Minimal noise

See: Hajj et al., 2002, Wickert et al., 2002, Beyerle et al., 2005, Schreiner et al., 2009

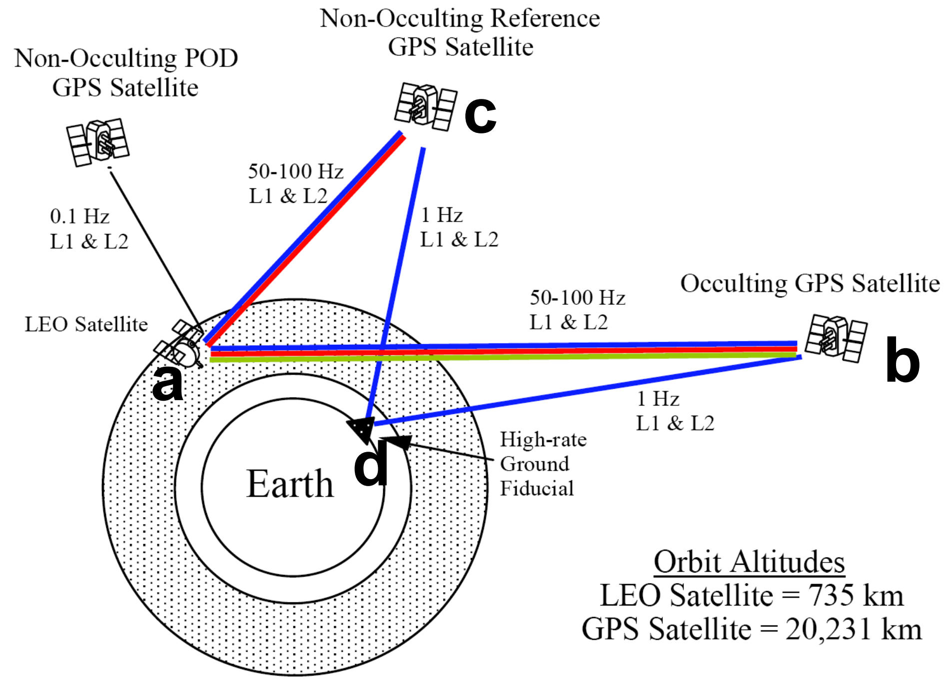

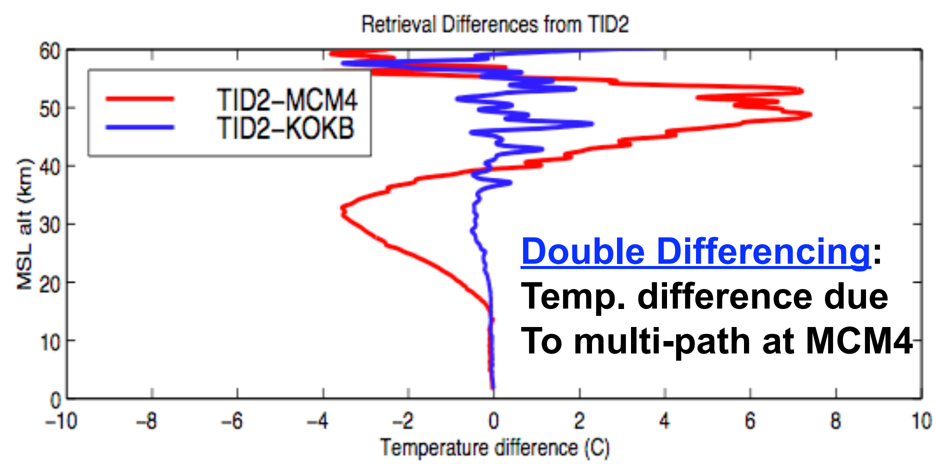

Single-Difference details

$$L1_a^b(t_r) = \boxed{c \cdot \delta t_a(t_r) + c \cdot \delta t_{a,rel}(t_r)} + \rho_a^b(t_r) + c \cdot \delta t^b(t_r - \tau_a^b) + c \cdot \delta t_{rel}^b(t_r - \tau_a^b) + \delta\rho_{a,rel}^b(t_r) + \boxed{\delta\rho_{a,ion}^b(t_r) + \delta\rho_{a,trop}^b(t_r)}$$

Subtract ionosphere-free reference link phase, and eliminate other terms to get:

$$L1_a^b(t_r) - L3_a^c(t_r) = \delta\rho_{a,ion}^b(t_r) + \delta\rho_{a,trop}^b(t_r)$$

Smooth reference link L1-L2 to reduce L2 noise, but increases the uncorrected small-scale ionospheric effects (Rocken et al., 1997, Schreiner et al., 1998, Beyerle et al., 2005)

For L1, use $$L3_a^c(t_r) = L1_a^c(t_r) + c_2\left\langle L1_a^c(t_r) - L2_a^c(t_r)\right\rangle$$

For L2, use $$L3_a^c(t_r) = L2_a^c(t_r) + c_1\left\langle L1_a^c(t_r) - L2_a^c(t_r)\right\rangle$$

$\langle\ \rangle$ denotes smoothing with a 2 sec window

In future for COSMIC L2 excess phase, use

$$L3_a^c(t_r) = L1_a^c(t_r) + c_2\left\langle L1_a^c(t_r) - L2_a^c(t_r)\right\rangle$$

Raw L1 Phase

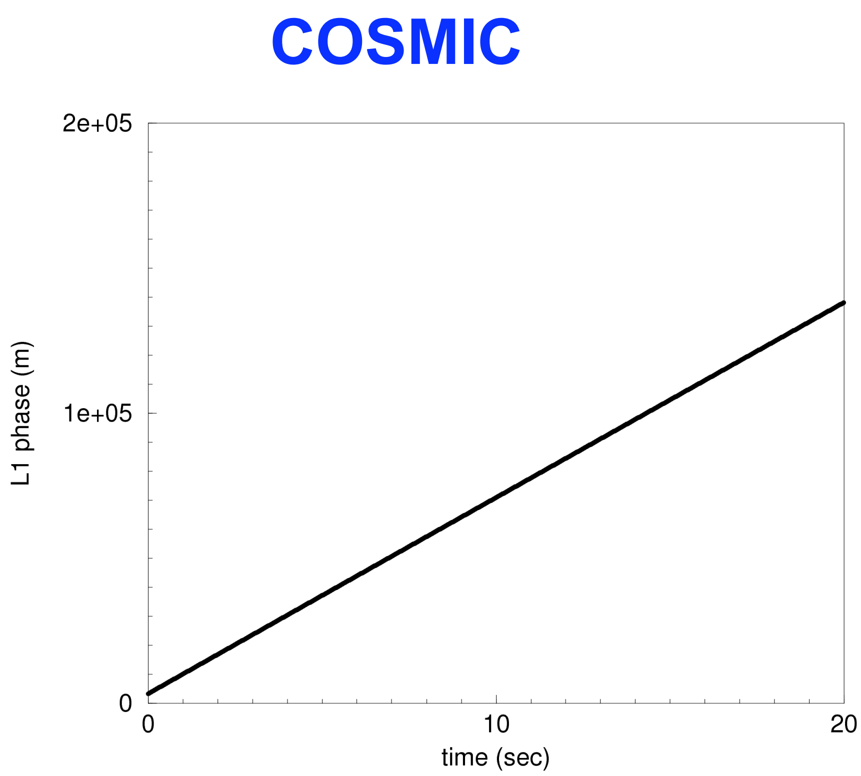
COSMIC
2e+05
1e+05
0
L1 phase (m)
0
10
20
time (sec)

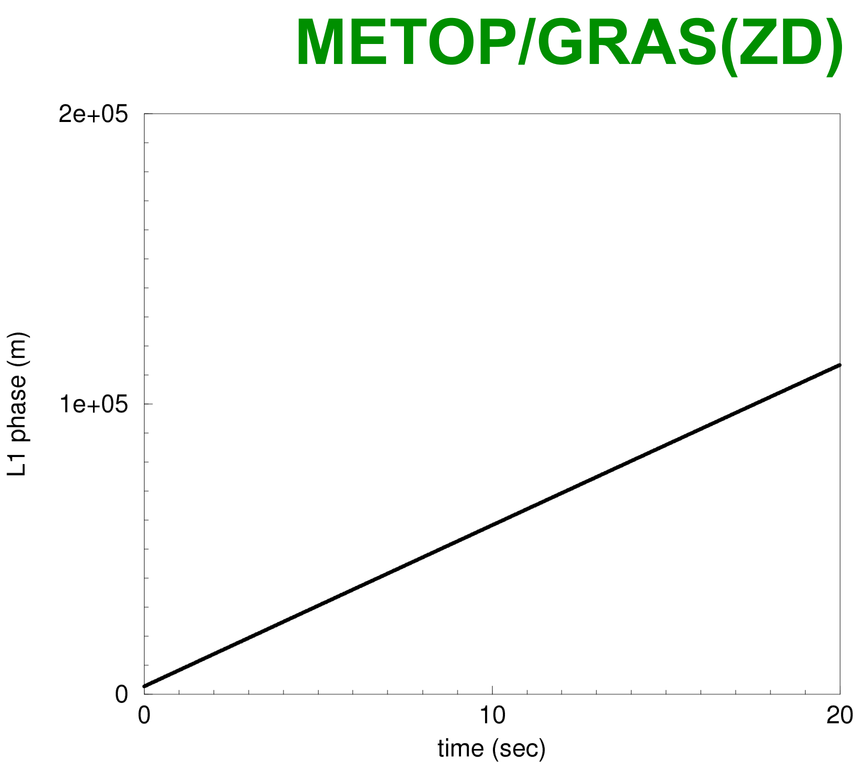
METOP/GRAS(ZD)
2e+05
1e+05
0
L1 phase (m)
0
10
20
time (sec)

Raw L1 Phase – Orbital Motion

COSMIC

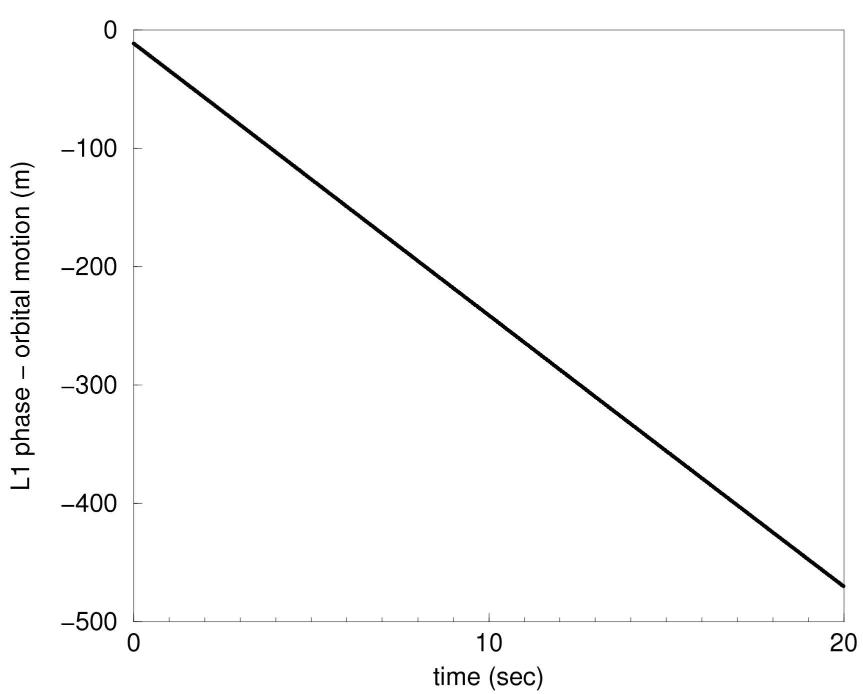

METOP/GRAS(ZD)

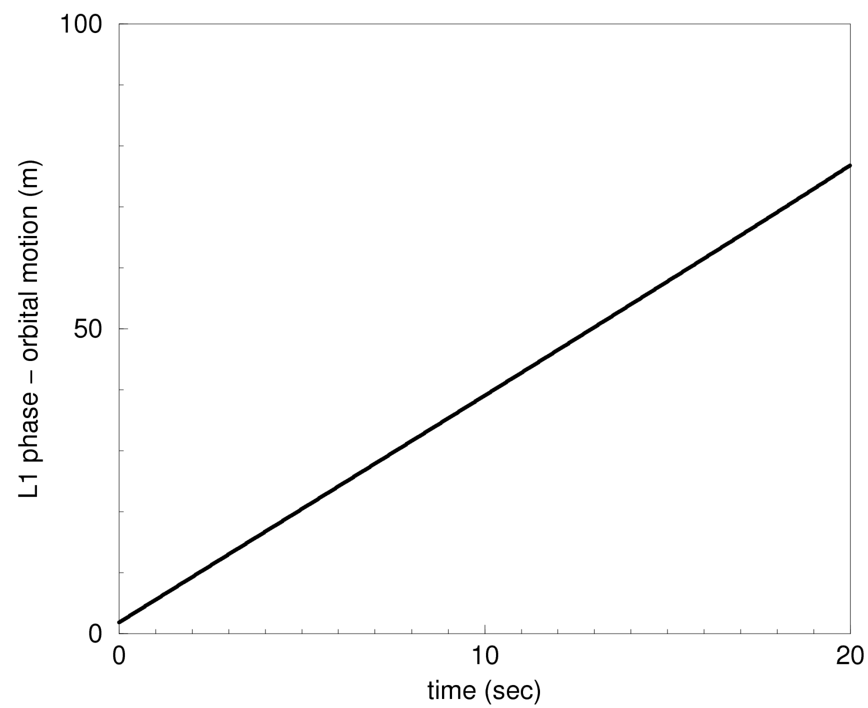

Subtract LEO and GPS clocks

COSMIC

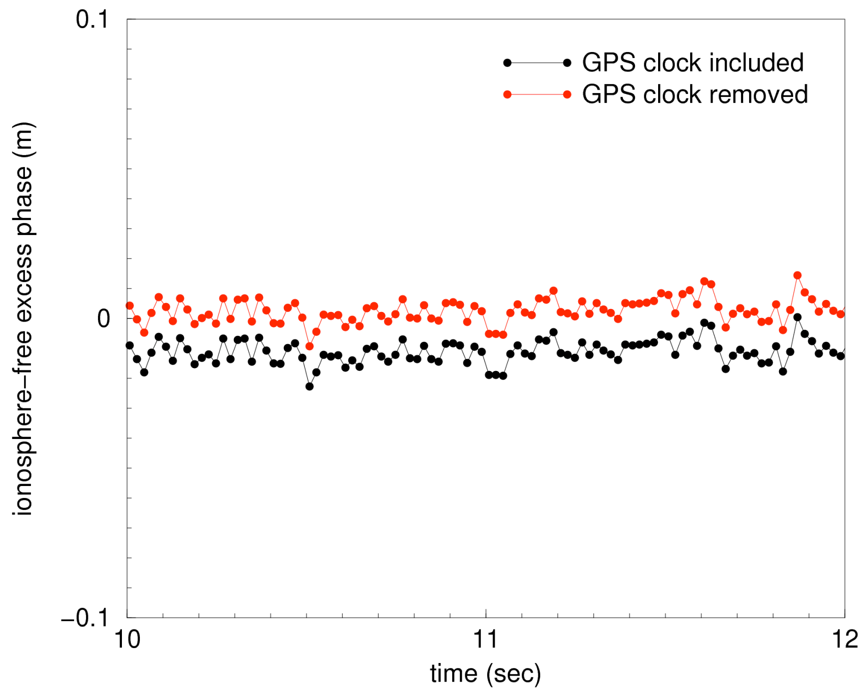

METOP/GRAS(ZD)

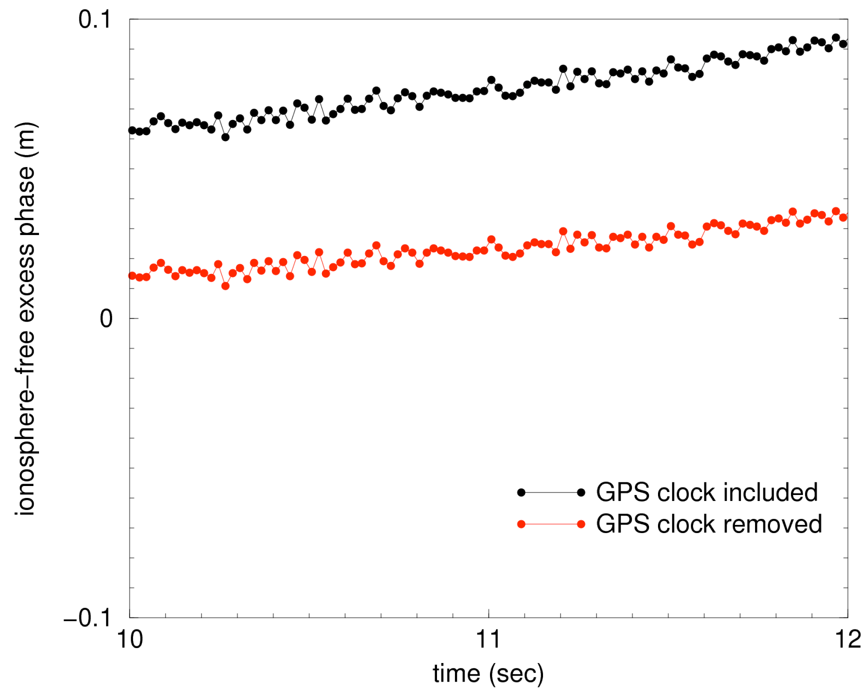

Bending angles from geometric optics

Geometric optics (GO) method - <u>uses phase</u>; needs single path propagation; provides accurate solutions in the UT and above; does not work in the LT.

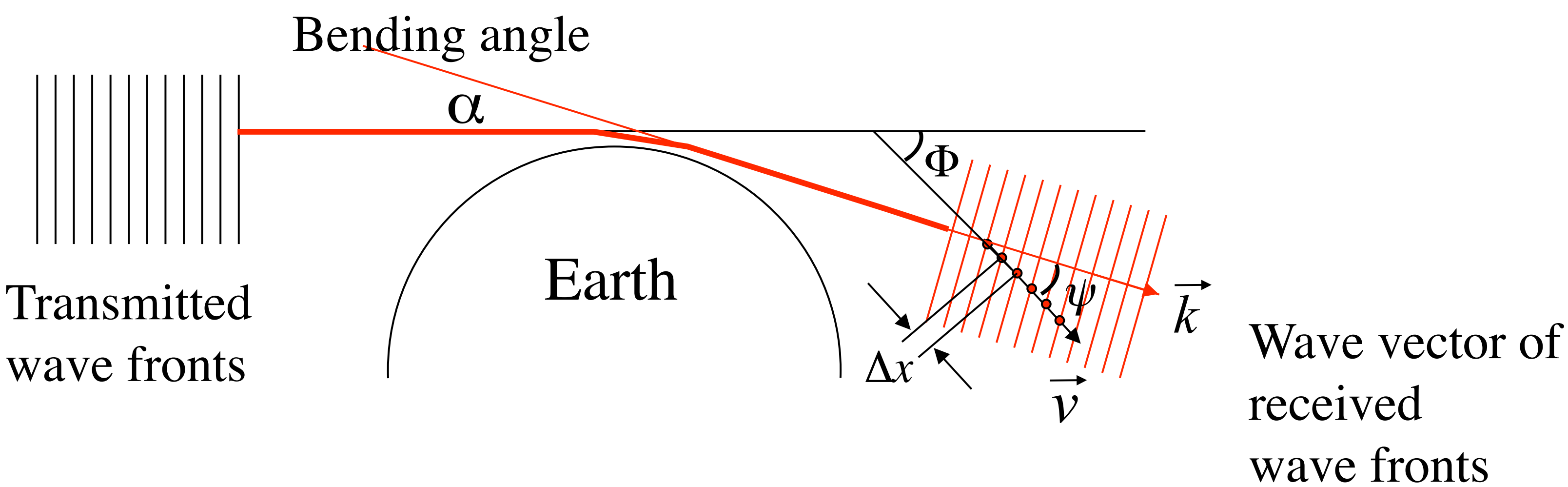

From orbit determination we know the location of source and We know the receiver orbit $\vec{v}$. Thus we know Φ

We measure Doppler frequency shift: $f_d = \dfrac{1}{\Delta t} = \dfrac{v}{\Delta x} = \dfrac{v}{\lambda}\cos\psi = f_T \dfrac{v}{c}\cos\psi$

Thus we know ψ. And compute the bending angle $\alpha = \Phi - \psi$

See Kursinski et al., JGR, 1997.

Ionospheric correction of bending angles

Ionospheric correction is performed on L1 and L2 bending angles by taking them at the same impact parameter (Vorob'ev and Krasil'nikova, 1994)

$$\alpha(a) = c_1\alpha_1(a) - c_2\alpha_2(a); \quad c_1 = f_1^2/(f_1^2 - f_2^2); \quad c_2 = f_2^2/(f_1^2 - f_2^2)$$

Alternatively, it can be performed: $\alpha(a) = \alpha_1(a) - c_2 < \alpha_4(a) >; \alpha_4 = \alpha_1 - \alpha_2$

The additional smoothing <> reduces the effect of larger noise on L2 (but increases the uncorrected small-scale ionospheric effects).

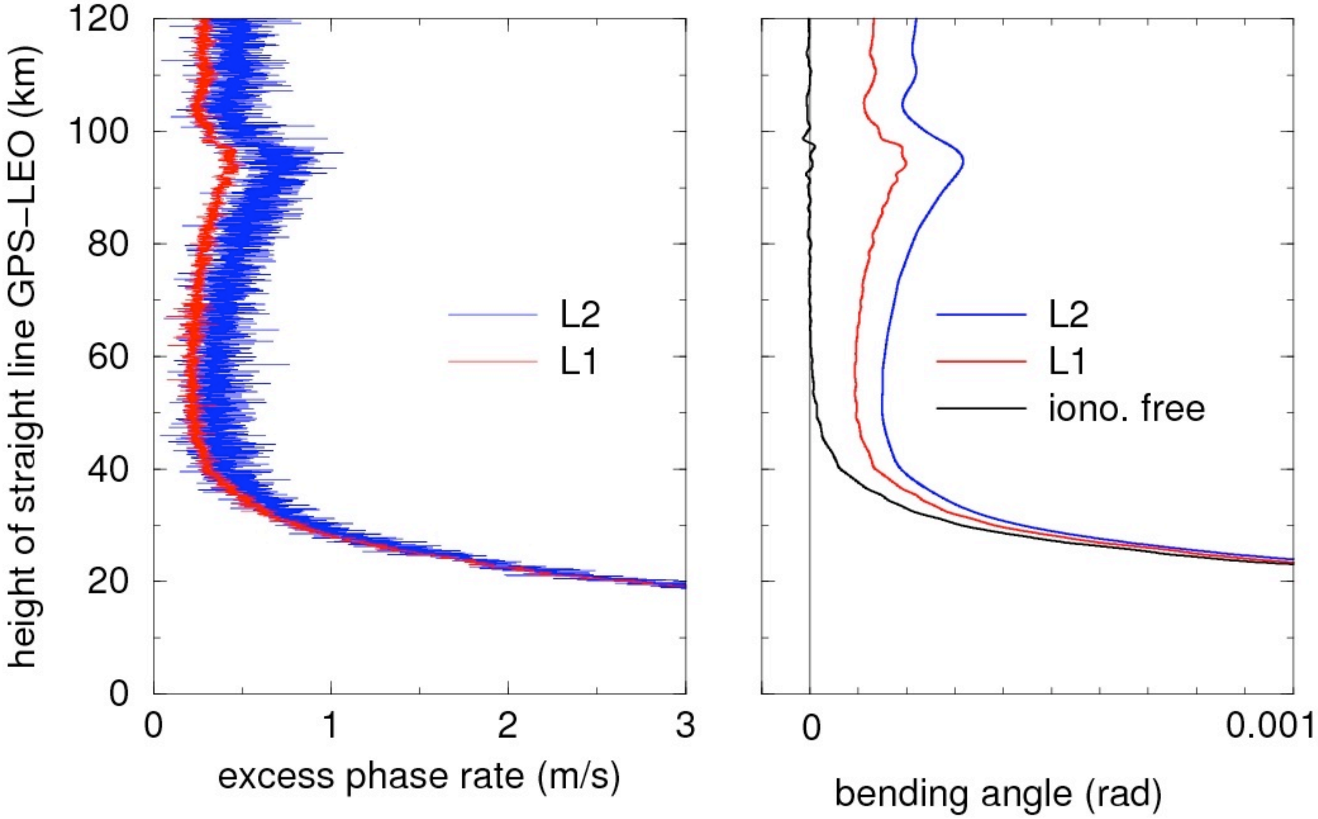

Optimal L4=L1-L2 filtering for the ionospheric correction

L2 noise is different in different occultations. The fixed window for L4 filtering is not optimal.
An optimal window is determined individually for each occultation.
Criterion: minimum LC fluctuation between 60 and 80 km.

Sokolovskiy et al., GRL, 2009

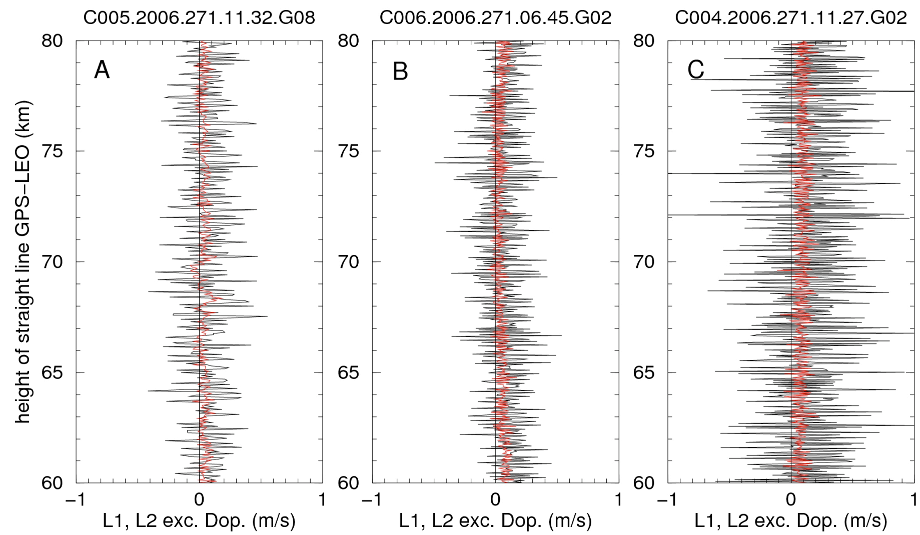

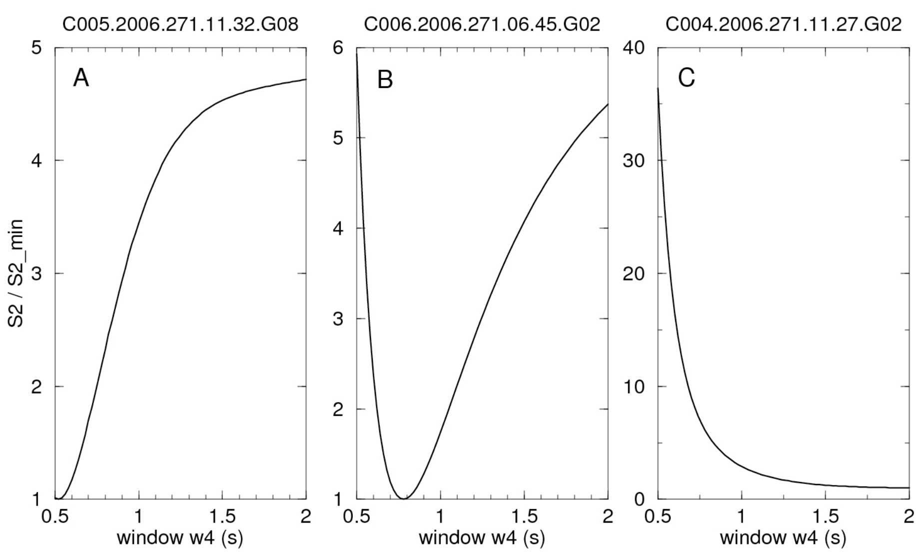

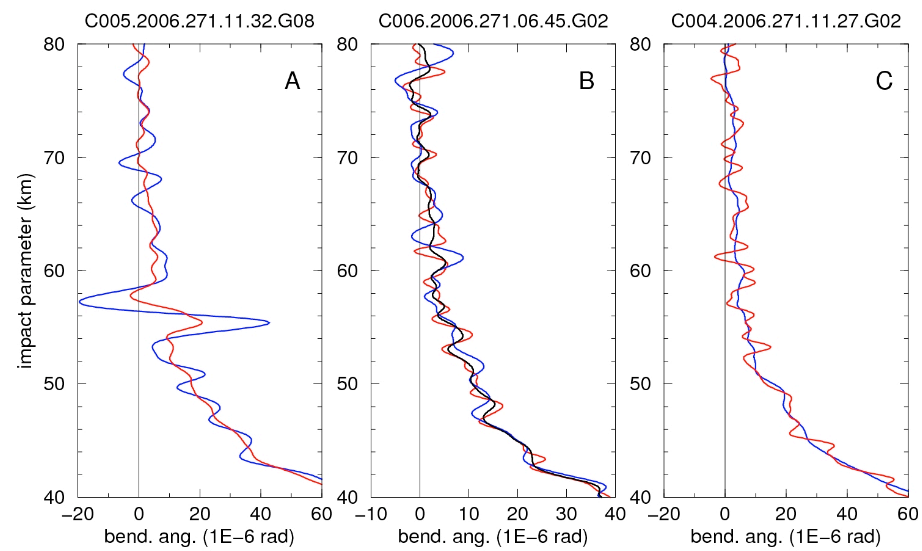

Bending angle noise between 60 and 80 km

- UCAR/CDAAC results
- 2007.274-283
- BA Noise (STDV) = rms deviation of the observed bending angle from the 1st guess between 60 and 80 km
- Discard outliers with STDV > 1e-5 rad. ~1%, many due to sporadic E clouds (Zeng and Sokolovskiy, 2010, GRL, in press)

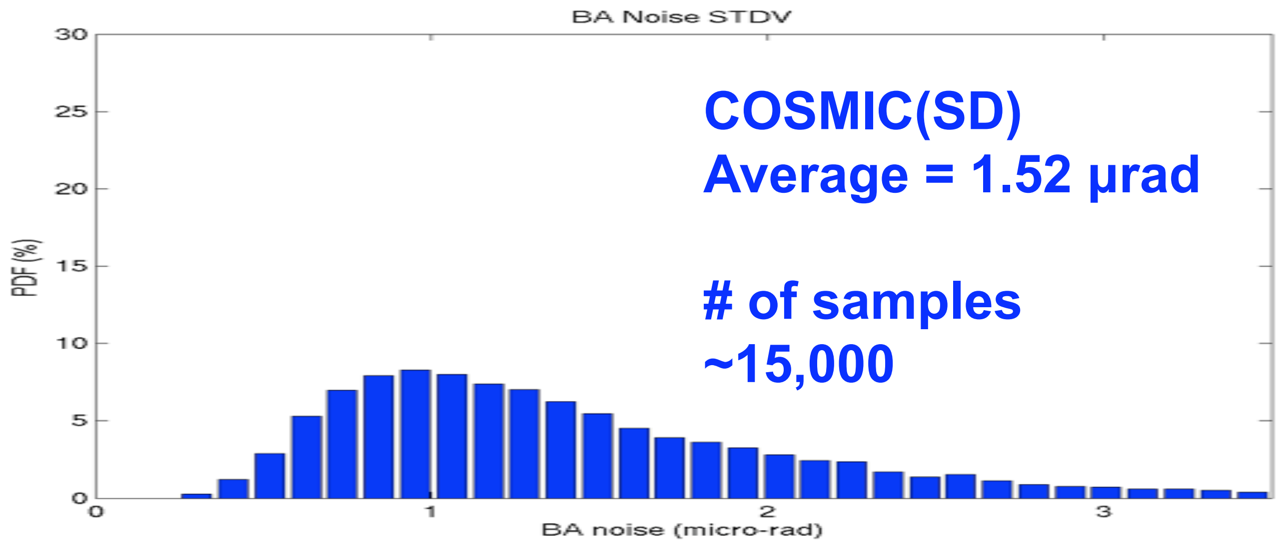

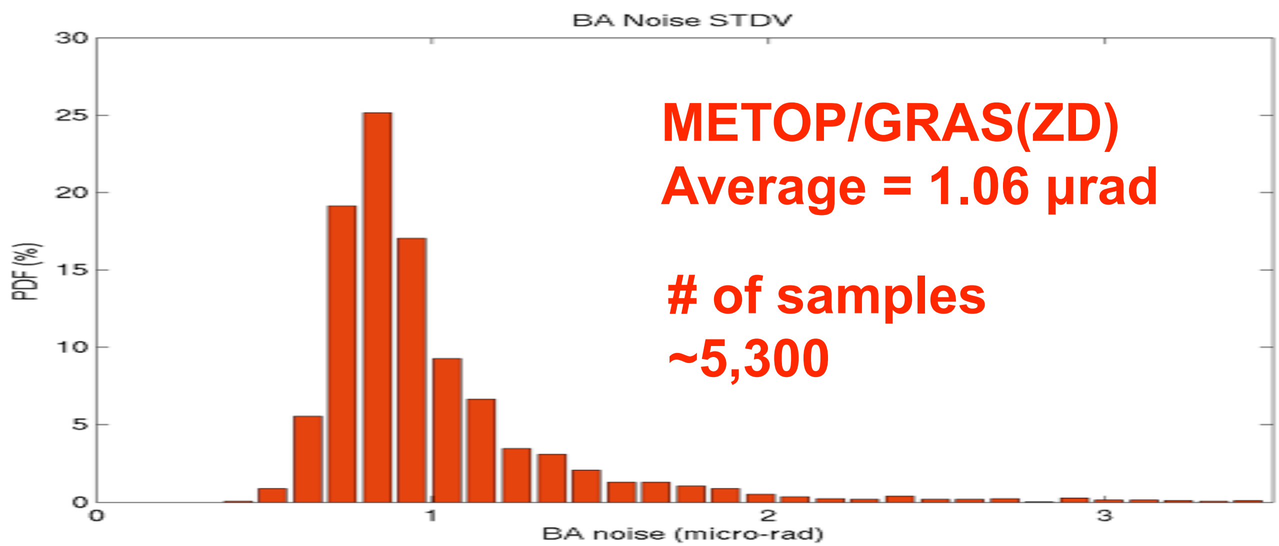

Bending angle noise

- **METOP/GRAS(SD)**
- **COSMIC(SD)**
- 2007.274-283
- Discard STDV > 1e-5 rad (~1%)

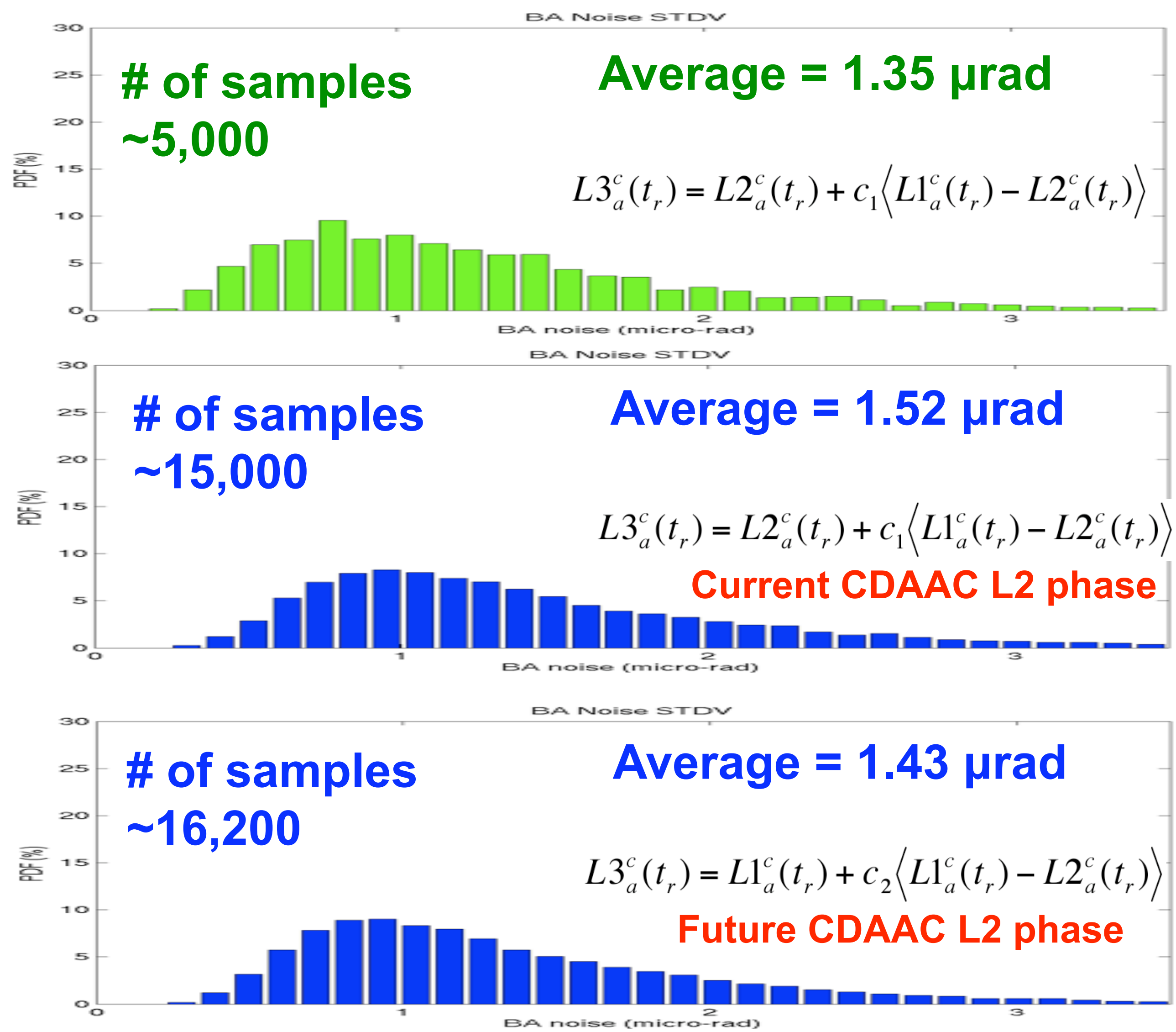

Bending angle noise vs. reference link L1-L2 smoothing

- **COSMIC(SD)**
- 2007.274-283
- Discard STDV > 1e-5 rad (~1%)

Used less noisy reference link for L2

$$L3_a^c(t_r) = L1_a^c(t_r) + c_2\left\langle L1_a^c(t_r) - L2_a^c(t_r)\right\rangle$$

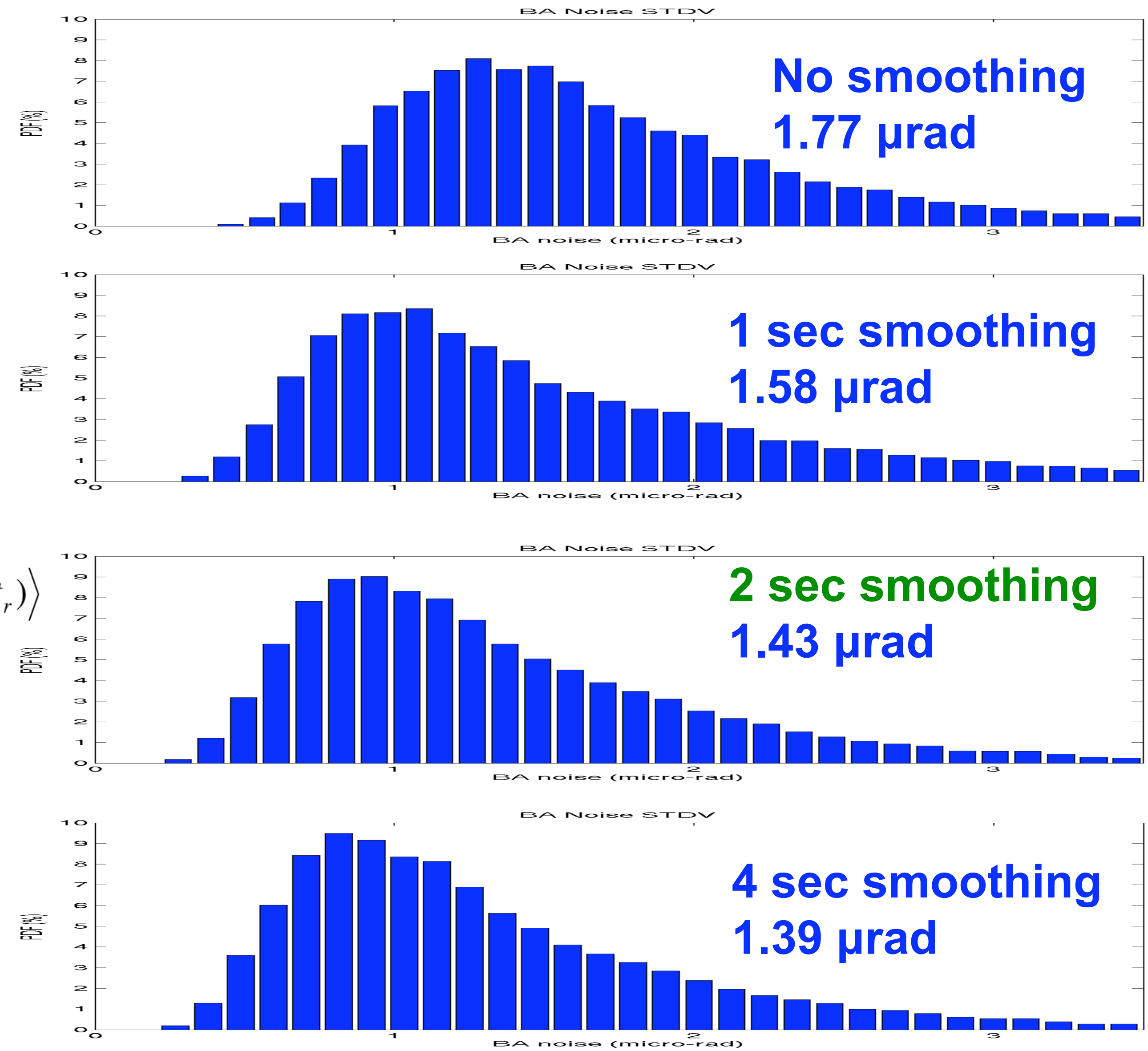

Bending angle mean between 60 and 80 km

COSMIC and METOP/GRAS(ZD): 2007.274-283

- BA Mean (SMEAN) = mean difference of the observation bending angle from the 1st guess between 60 and 80 km
- Discard |SMEAN| > 3.5e-6 rad (~1%)

Different averages are significant - May be due to large scale ionospheric residuals that are a function of local time.

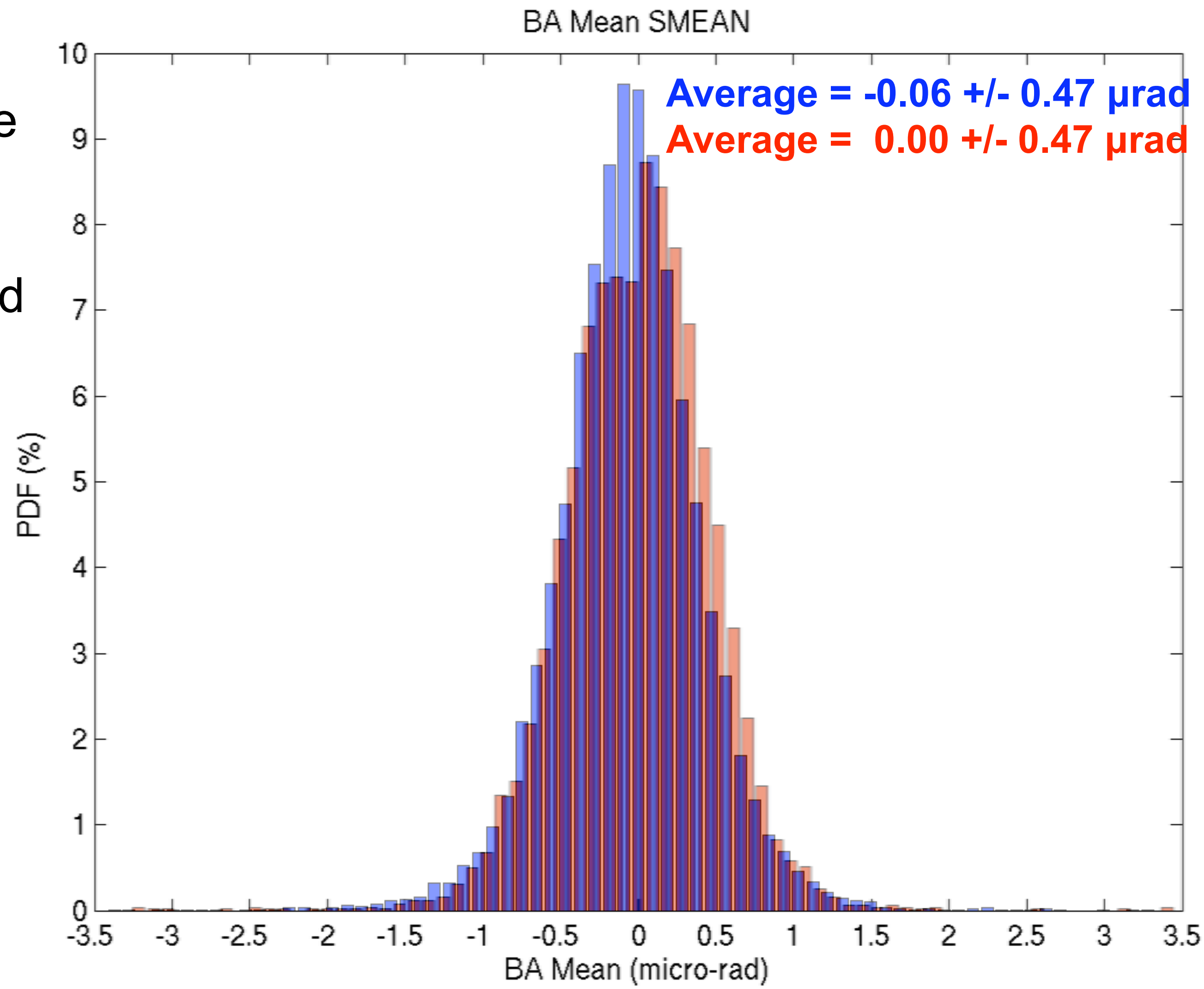

Systematic Bending Angle Differences COSMIC VS Metop/GRAS

(~10,000 Collocations within 2 hours/300 km, Jun-Dec 2009)

- Bending angle bias between 40 and 60km ~ -3e-8 +/- 3e-8 rad
- May be due to old version of Metop/GRAS processing?
- **3e-8 rad translates into ~0.04 K (0.02%) at 20 km altitude**

COSMIC (Single Difference) – Metop/GRAS Beta (Zero Difference)

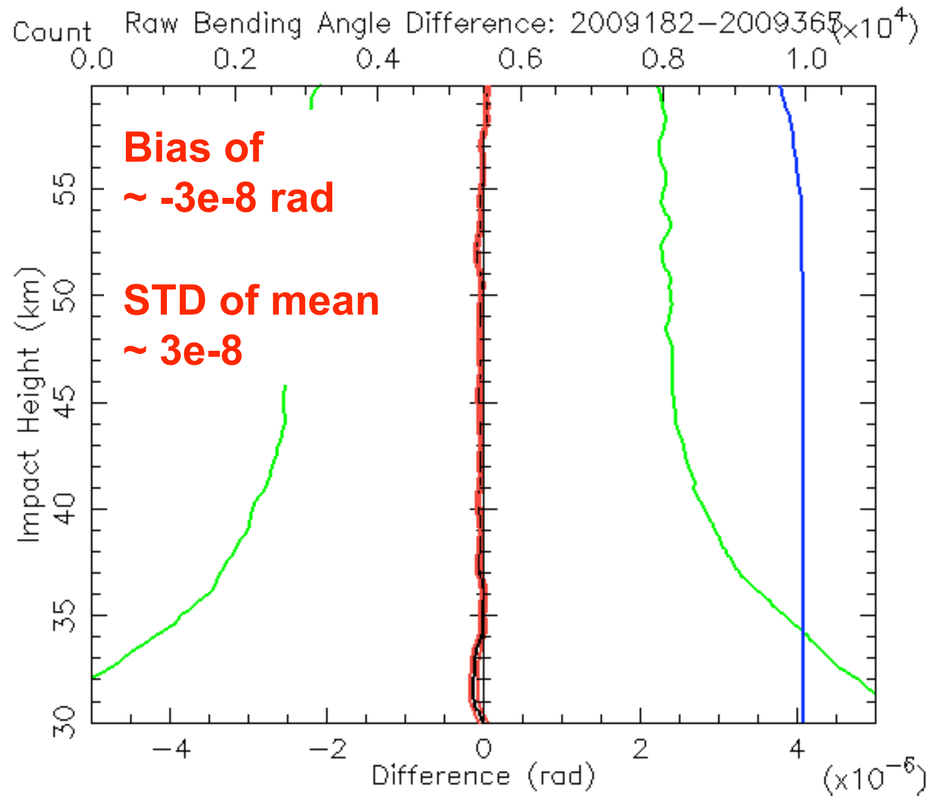

Schreiner et al., AMS, 2010

Progress in inversion methods (derivation of bending angles from RO signals under the assumption of local spherical symmetry)

Wave optics (WO) methods - use phase & amplitude; solve for the multipath propagation in LT:

back propagation (BP) - propagates complex wave field measured on the observation trajectory back to limb (in the single-path region), then calculates bending from phase.
sliding spectral (SS) methods - perform spectral analysis of the measured wave field in a sliding aperture to identify multiple rays and estimate their bending angles.
Most advanced WO methods are based on integral transform of the whole measured RO signal from coordinate to impact parameter representation:
canonical transform (CT, Gorbunov 2002**); full spectrum inversion (FSI,** Jensen at al. 2003**); phase matching (PM,** Jensen at al. 2004**);**
canonical transform 2 (CT2, Gorbunov and Lauritsen 2004**)**
CT - uses BP to straight line
FSI, CT2 - use representations of approximate impact parameter
FSI, CT2 - are computationally efficient (reduce to FFT, do not use BP)
PM - can be used for verification of other methods

The difference between inversion results obtained with CT, FSI, PM, CT2 is much smaller than other errors of RO in LT

Comparison of the Full Spectrum Inversion (FSI) and Phase Matching (PM)

Tropical occultation. Strong fluctuation of the amplitude of transformed signal. Cycle slips possible.

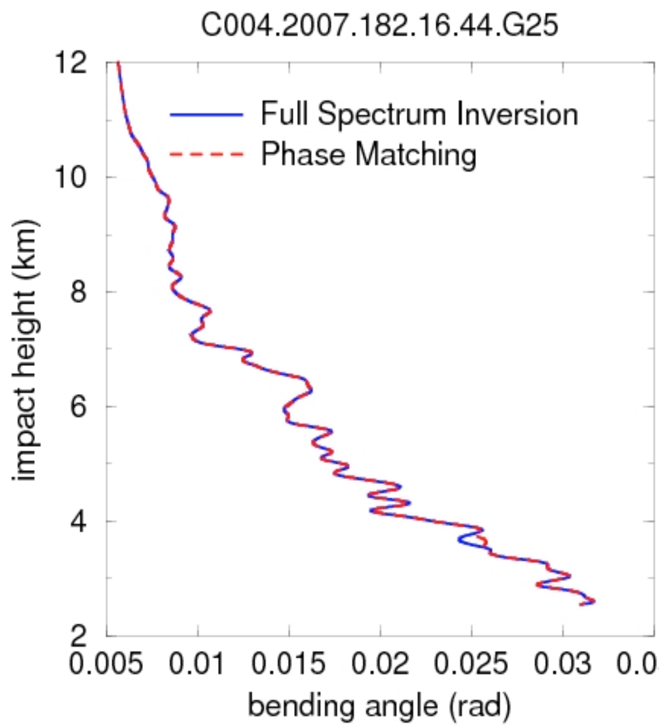

Statistical comparison COSMIC - ECMWF

FSI

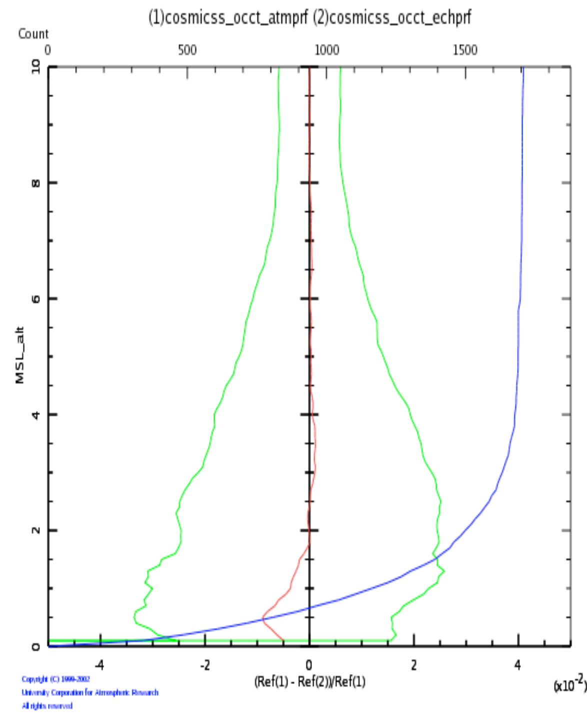

PM

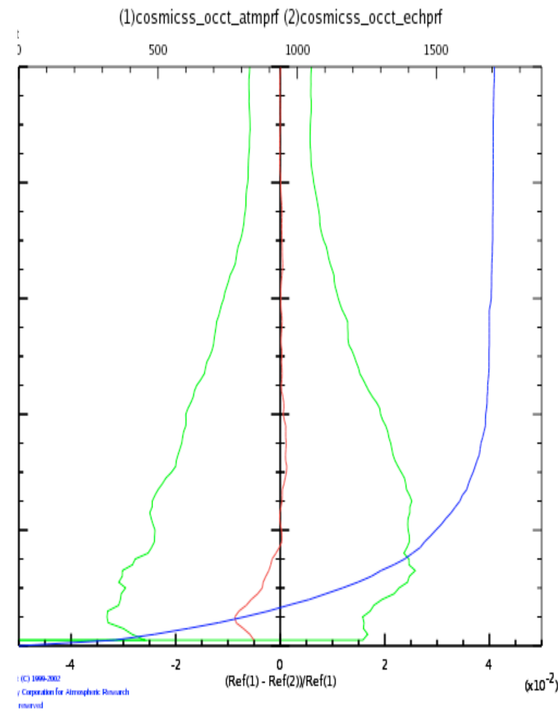

The use of one or another WO method (FSI or PM) does not introduce noticeable difference in BA. However, there are other reasons for uncertainty (see next slides).

Upper stratosphere and lower troposphere are regions of the maximum uncertainty of the GPS RO inversions

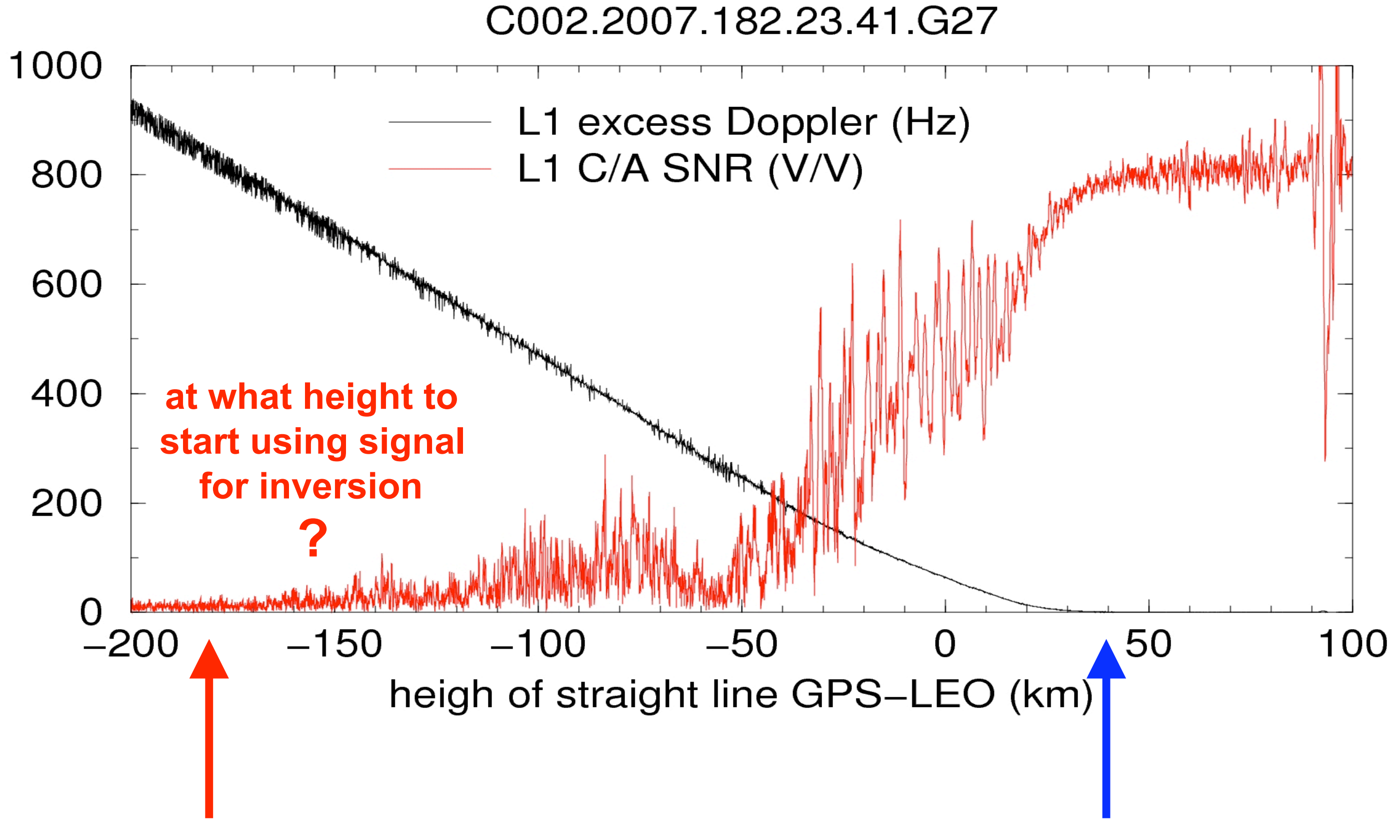

In the lower troposphere:
the signal reduces below noise level in terms of the amplitude

In the upper stratosphere:
the signal reduces below noise level in terms of the phase (Doppler)

Reasons for the uncertainty (inversion biases) in LT:

Atmosphere:

- ducting - results in the **negative bias** (RO signals propagate very deep)
- moist convection - breaks condition of applicability of WO methods by broadening the local spectrum of WO-transformed signal and making the determined frequency (BA) susceptible to local distribution of noise (may introduce both positive and negative bias)

Important: changing structure of the moist LT may result in changing of the inversion biases (and thus aliasing into the total retrieved N, water vapor)

Receiver:

- tracking depth - insufficient depth results in missing of sub-signals with largest BA **(negative bias)** (see above)
- noise level - with 50 Hz sampling, local distribution of noise is asymmetric around WO-transformed signal (may introduce both **positive** and **negative** inversion bias)

Inversion:

- truncation of raw signal - high truncation removes the sub-signals with largest BA (**negative bias**); low truncation passes more noise (**positive bias**)
- filtering - RH filtering of the WO-transformed signal reduces positive bias induced by the noise and introduces negative bias due to suppression of sub-signals with largest BA

Sokolovskiy et al., JGR 2010 (in press)

Observed signal: noise band has given frequency width.

WO-transformed signal: noise band has given impact height width.

Distribution of noise wrt mean frequency becomes asymmetric.

The asymmetry results in the bias (negative near the cut-off, positive above) when local spectrum of the WO-transformed signal is broad.

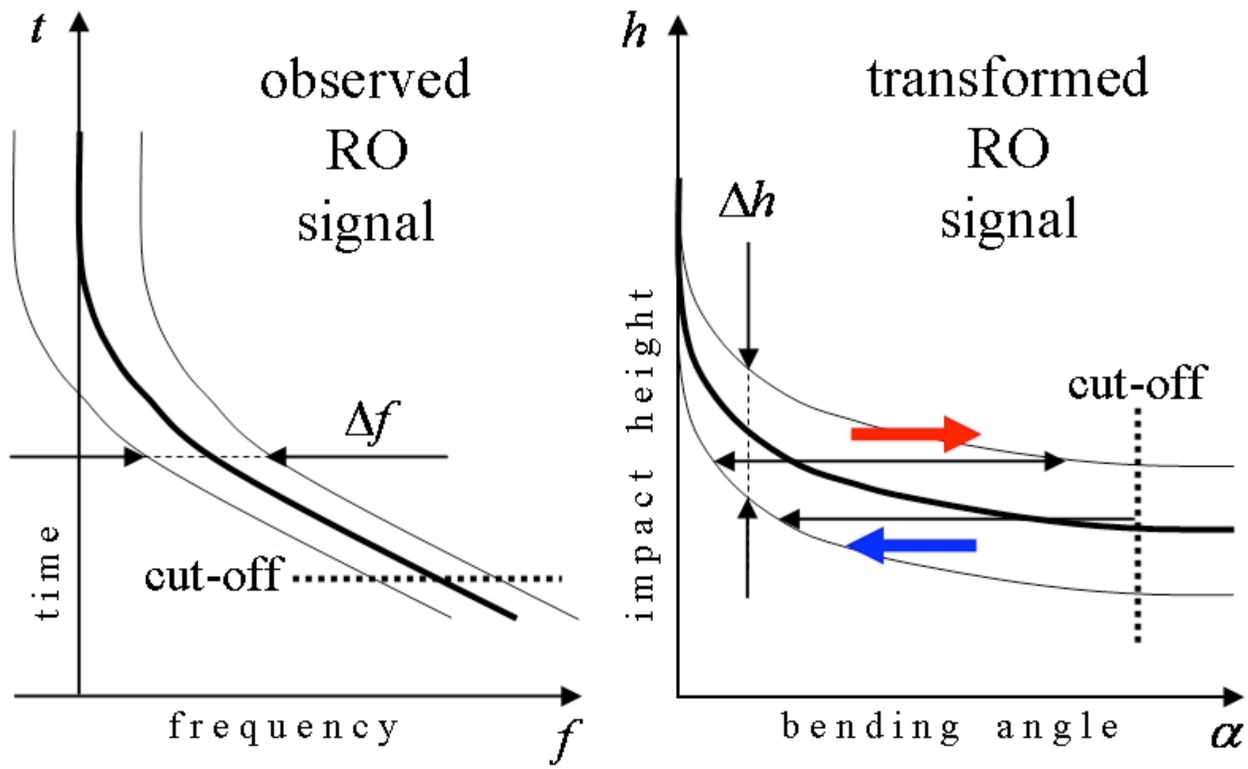

With the 50 Hz sampling, local spectrum of noise of the WO-transformed RO signal is asymmetric. The asymmetry increases with the increase of the length of RO signal.

High latitudes:
WO-transformed RO signal has narrow local spectrum. The asymmetry of the local spectrum of noise does not affect determination of the frequency (BA).

Low latitudes:
WO-transformed RO signal has broad local spectrum. The asymmetry of the local spectrum of noise introduces bias in the determined frequency (BA).
RO signal used down to low HSL - positive bias.
RO signal truncated high - negative bias (at the bottom).

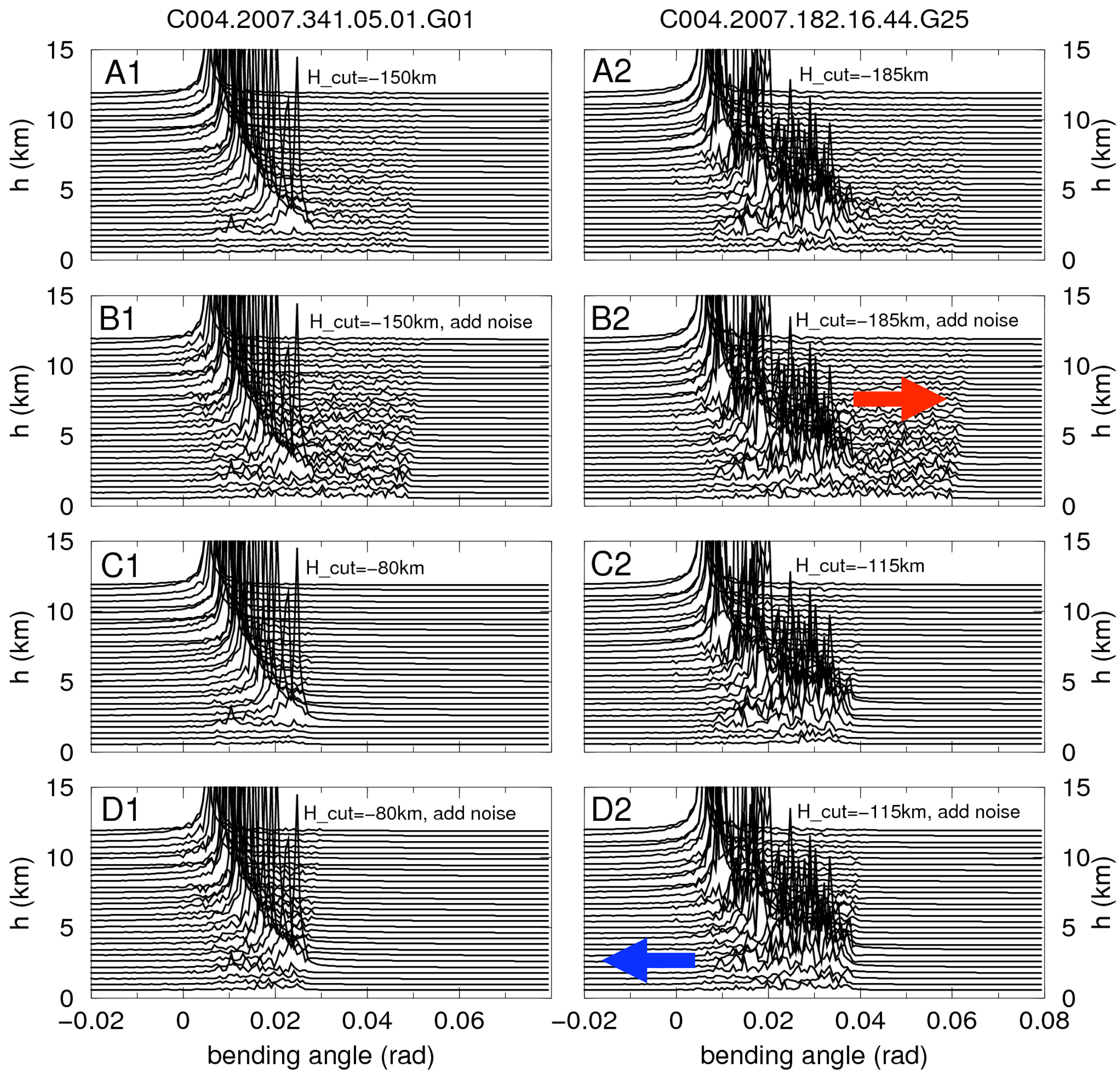

Inversion biases

Truncation of RO signal with large BA (sharp ABL top in sub-tropics) results in the negative bias at and below the ABL top.

Imposing additional noise when local spectrum of WO-transformed signal is broad (moist convection in tropics) introduces positive inversion bias when the full signal is used; negative bias for truncated signal.

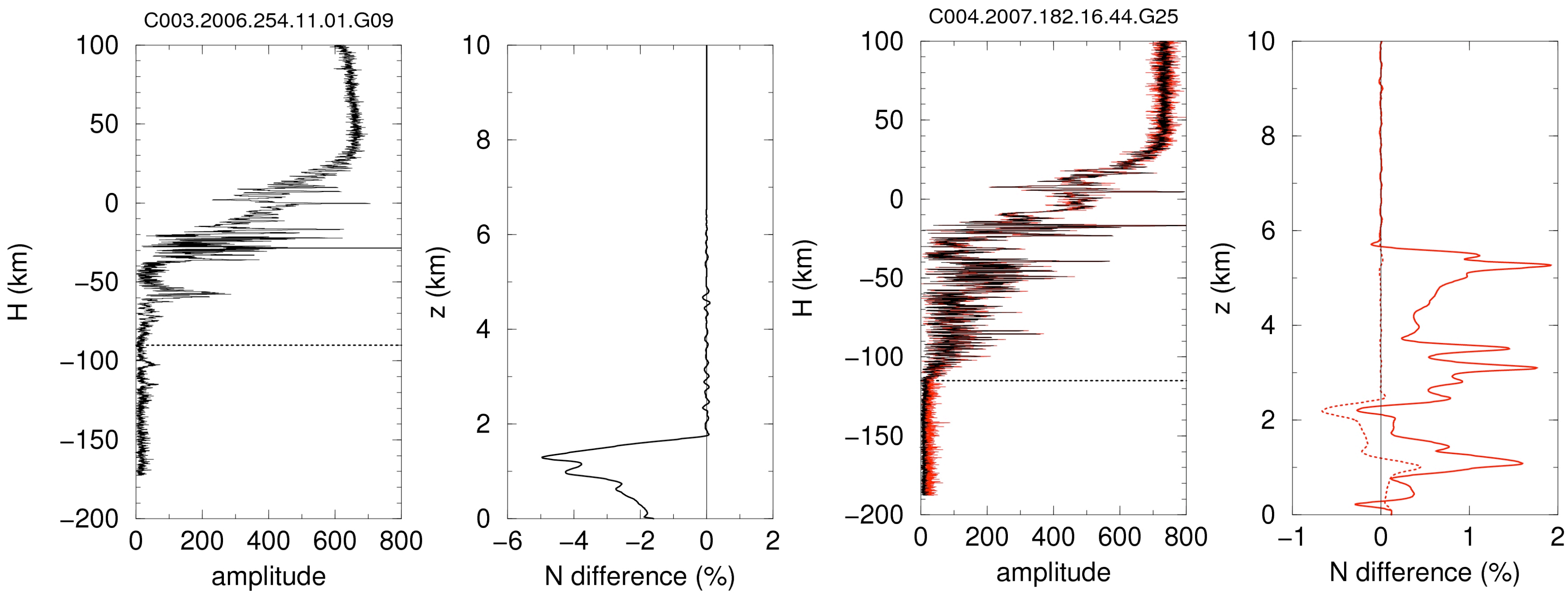

Difference in the inversion N-bias (COSMIC - ECMWF) for different cut-off heights HSL= -100 km and HSL= -150 km with (dashed lines) and without (solid lines) additional noise. Higher truncation: larger negative bias. Lower truncation: larger positive bias induced by noise.

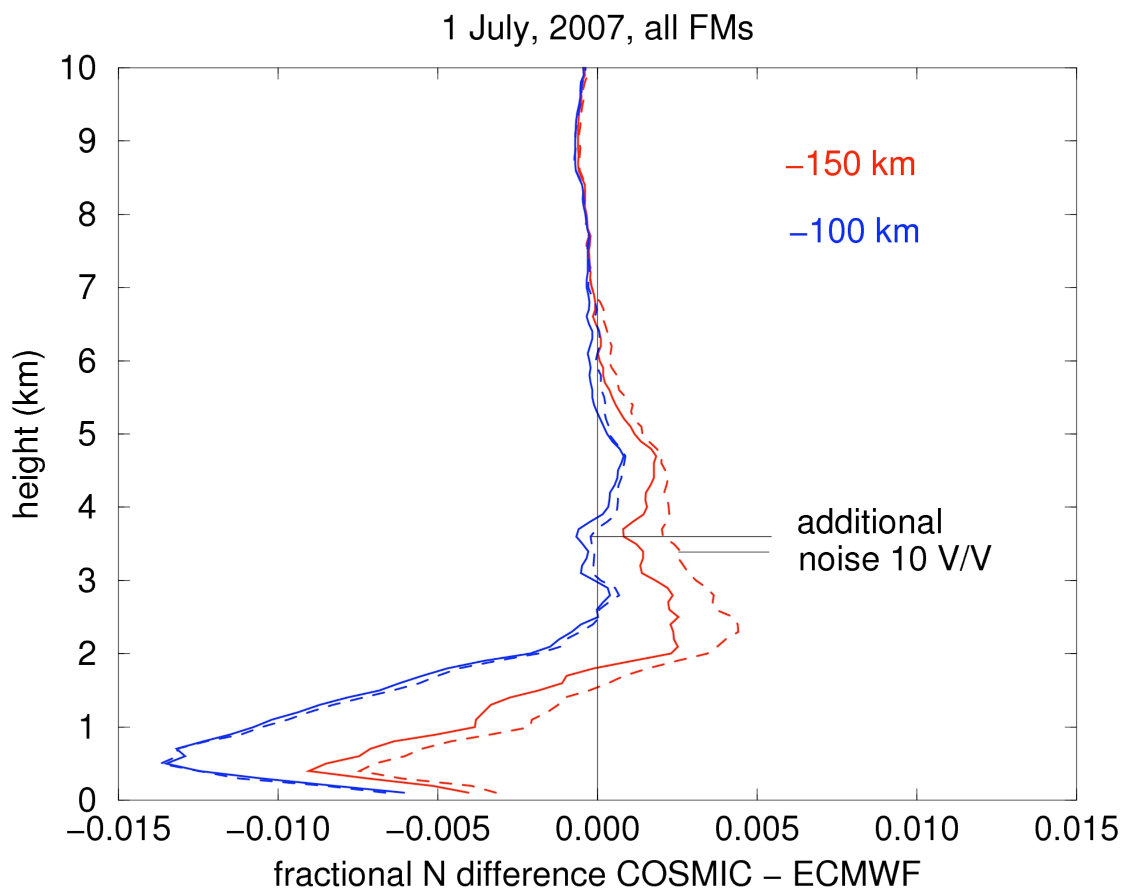

Difference in the inversion N-bias (COSMIC - ECMWF) for different SNR with and without the RH filtering (Gorbunov, Lauritsen, et al., 2004, 2006) . The RH filtering reduces the inversion difference between high- and low-noise occultations, but results in the mean negative difference.

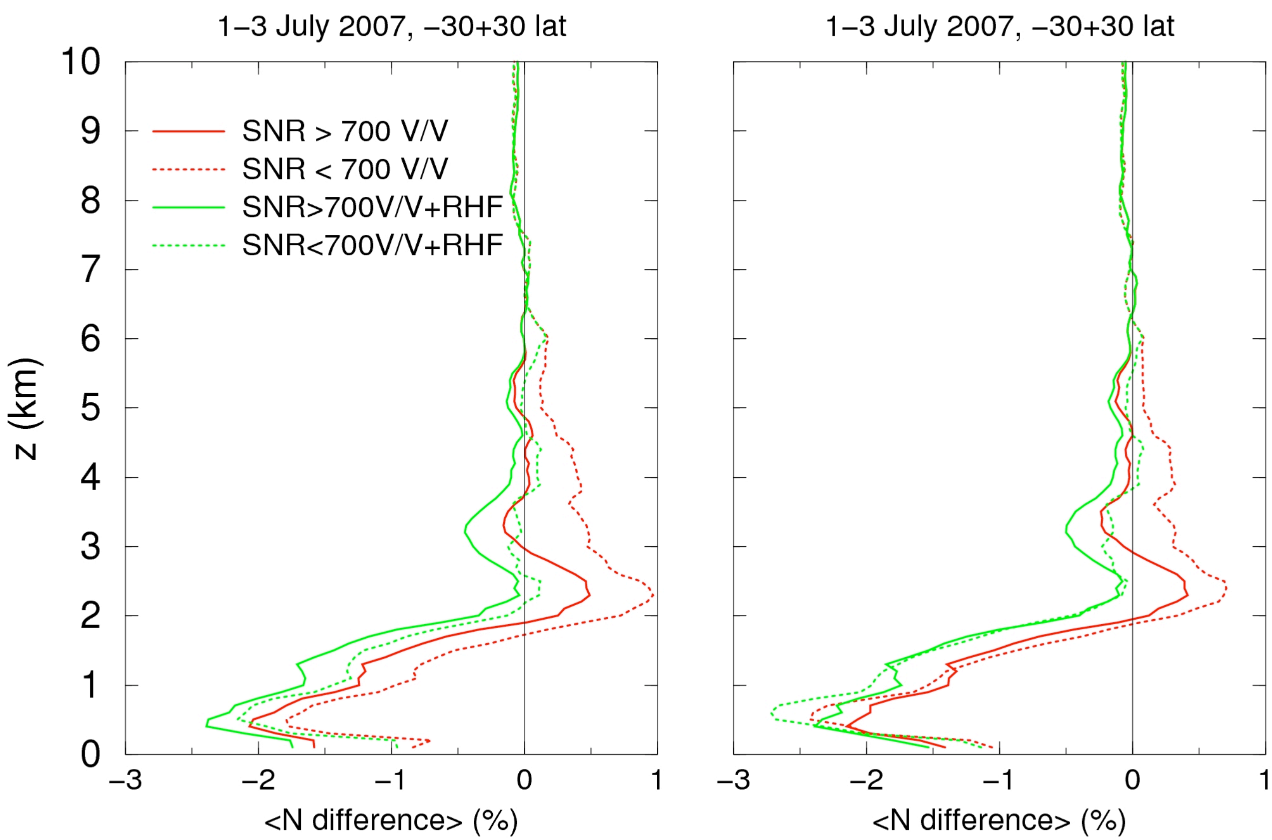

fixed cut-off at HSL=-150 km

"dynamic" cut-off (at HSL where amplitude exceeds background noise value)

Summary

- ZD processing produces less BA noise than SD
- Smoothing reference link L2 more doesn't significantly reduce BA noise
- COSMIC and METOP/GRAS SD have similar BA noise
- COSMIC mean BA is slightly smaller than METOP/GRAS
- Atmospheric ducting results in the **negative bias**
- Insufficient tracking depth and high truncation of raw signal result in **negative bias**
- Local distribution of noise is asymmetric around WO-transformed signal and may introduce both **positive** and **negative** inversion bias
- In moist LT, RH filtering of the WO-transformed signal reduces **positive** bias induced by the noise and introduces **negative** bias due to suppression of sub-signals with largest BA
- changing structure of the moist LT may result in changing of the inversion biases

UCAR COMMUNITY PROGRAMS

Acknowledgments

COSMIC

- U.S. National Science Foundation
- Taiwan’s NSPO
- NASA/JPL, NOAA, USAF, ONR, NRL
- Broad Reach Engineering
- EUMETSAT

UCAR NSF NASA USAF NOAA NSPO ONR

BROAD REACH ENGINEERING
www.broadreachengineering.com Spaceflight Hardware, Software, Vehicle Design

References

Beyerle, G., T. Schmidt, G. Michalak, S. Heise, J. Wickert, and C. Reigber, (2005) GPS radio occultation with GRACE: Atmospheric profiling utilizing the zero difference technique, *Geophys. Res. Lett.*, 32, L13806, doi: 10.1029/2005GLo23109.

Gorbunov, M.E. (2002), Canonical transform method for processing radio occultation data in the lower troposphere, Radio Sci. 37(5), 1076, doi:10.1029/2000RS002592.

Gorbunov, M.E. and K.B. Lauritsen (2004), Analysis of wave fields by Fourier integral operators and their application for radio occultations, Radio Sci., 39, RS4010, doi:10.1029/2003RS002971.

Hajj, G. A., E. R. Kursinski, L. J. Romans, W. I. Bertiger, and S. S. Leroy (2002), "A technical description of atmospheric sounding by GPS occultation", *J. Atmos. Sol.-Terr. Phys.*, 64 (4), 451-469.

Jensen, A.S., M.S. Lohmann, H. Benzon, and A.S. Nielsen (2003), Full spectrum inversion of radio occultation signals, Radio Sci., 38(3), 1040, doi:10.1029/2002RS002763.

Jensen, A.S., M.S. Lohmann, A.S. Nielsen, and H. Benzon (2004), Geometric optics phase matching of radio occultation signals, Radio Sci., 39, RS3009, doi:10.1029/2003RS002899.

Kuo, Y. H. , T.-K. Wee, S. Sokolovskiy, C. Rocken, W. Schreiner, D. Hunt, R. A. Anthes, 2004: Inversion and Error Estimation of GPS Radio Occultation Data. J. Meteor. Soc. Japan, 82:5661, doi:10.2151/jmsj. 2004.507.

Kursinski, E.R., G.A. Hajj, J.T. Schofield, R.P. Linfield, and K.R. Hardy, Observing Earth's atmosphere with radio occultation measurements using the Global Positioning System, J. Geophys. Res 102 (D19), 23429-234651997, 1997.

Rocken, C., R. Anthes, M. Exner, D. Hunt, S. Sokolovskiy, R. Ware, M. Gorbunov, W. Schreiner, D. Feng, B. Herman, Y.-H. Kuo, and X. Zou, 1997: Analysis and validation of GPS/MET data in the neutral atmosphere, *J. Geophys. Res.*, 102, 29,849-29,860.

Schreiner, W., C. Rocken, S. Sokolovskiy, and D. Hunt, 2009: Quality assessment of COSMIC/FORMOSAT-3 GPS radio occultation data derived from single- and double-difference atmospheric excess phase processing. GPS Solutions, 14:1, 13-22, doi:10.1007/s10291-009-0132-5.

References

Schreiner, W.S., D.C. Hunt, C. Rocken, S. Sokolovskiy, "Precise GPS Data Processing for the GPS/MET Radio Occultation Mission at UCAR", proceedings of the Institute of Navigation - Navigation 2000, Long Beach, CA. 103-112. 21-23 January 1998.

Sokolovskiy, S., C. Rocken, W. Schreiner, and D. Hunt, 2010: On the uncertainty of radio occultation inversions in the lower troposphere. J. Geophys. Res., 2010JD014058 (in press).

Sokolovskiy, S., W. Schreiner, C. Rocken, and D. Hunt, 2009: Optimal Noise Filtering for the Ionospheric Correction of GPS Radio Occultation Signals. J. Atmos. Oceanic Technol., 26:7, 1398–1403.

Sokolovskiy, S., C. Rocken, W. Schreiner, D. Hunt, and J. Johnson, 2009: Post-processing of L1 GPS radio occultation signals recorded in open-loop mode. Radio Science, 44, RS2002, doi:10.1029/2008RS003907.

Sokolovskiy, S., C. Rocken, D. Hunt, W. Schreiner, J. Johnson, D. Masters, and S. Esterhuizen. 2006: GPS profiling of the lower troposphere from space: Inversion and demodulation of the open-loop radio occultation signals. Geophysical Research Letters, 33, L14816, doi:10.1029/2006GL026112.

Svehla, D.; Rothacher, M.: Kinematic and reduced-dynamic precise orbit determination of CHAMP satellite over one year using spaceborne GPS phase zero-differences only; Geophysical Research Abstracts, EGS-AGU-EUG Joint Assembly, Vol. 5, pp 287, EGU, ISSN 1029-7006, 2003.

Wickert J, Beyerle G, Hajj GA, Schwieger V, Reigber C, (2002) GPS radio occultation with CHAMP: Atmospheric profiling utilizing the space-based single difference technique, *GRL* 29(8), 10.1029/2001GL13982.

Zeng, Z. and S. Sokolovskiy, 2010: Effect of sporadic E clouds on GPS radio occultation signals. Geophys. Res. Lett., 2010GL044561 (in press).